Supplementary Information (SI) for Journal of Materials Chemistry A.
This journal is © The Royal Society of Chemistry 2026

Supplementary materials

Trace High-Entropy Doping Enabling High-Stability and High-Energy-Density Sodium-Ion Batteries

Yu-Xiong Qin [a, b], Zu-Tao Pan [a, b], Xuan-Xi Liu [a, b], Hao-Peng Lu [a, b], Lei Xian [a, b], Ling-Bin Kong [a, b,] *

a State Key Laboratory of Advanced Processing and Recycling of Non-ferrous Metals, Lanzhou University of Technology, Lanzhou 730050, P. R. China

b School of Materials Science and Engineering, Lanzhou University of Technology, Lanzhou 730050, P. R. China

* Corresponding author. E-mail: konglb@lut.edu.cn

Migration Pathway Characterization

The migration energy barrier was computed using the Bond-Valence Potential Analysis (BVPA) method implemented in the softBV-GUI. [1]

Space Group = P6$_3$/mmc		**R_p = 6.97%**		**R_{wp} = 9.27%**		
					χ^2 = 1.79	
a(Å) = b(Å) = 2.88782		**c(Å) = 11.1524**		**V(Å^3) = 80.545**		
Atom	**Wyckoff Position**	**x**	**y**	**z**	**Occuapncy**	**U_{ios}**
O	4f	0.66667	0.33333	0.09438	1	0.04
Nae	6h	0.26707	0.53415	0.25	0.15	0.036
Naf	2b	0	0	0.25	0.221	0.065
Mn	2a	0	0	0	0.667	0.025
Ni	2a	0	0	0	0.333	0.025

Table S1. Detailed Rietveld refinement results of the XRD pattern for NM.

Space Group = P6$_3$/mmc		**R_p = 5.92%**		**R_{wp} = 7.71%**		
					χ^2 = 1.63	
a(Å) = b(Å) = 2.89219		**c(Å) = 11.1634**		**V(Å^3) = 80.869**		
Atom	**Wyckoff Position**	**x**	**y**	**z**	**Occuapncy**	**U_{ios}**
O	4f	0.66667	0.33333	0.07805	1	0.032
Nae	6h	0.36119	0.72237	0.25	0.143	0.052
Naf	2b	0	0	0.25	0.241	0.077
Mn	2a	0	0	0	0.62	0.009
Ni	2a	0	0	0	0.28	0.009
Mg	2a	0	0	0	0.025	0.009
Zn	2a	0	0	0	0.025	0.009
Zr	2a	0	0	0	0.05	0.009

Table S2. Detailed Rietveld refinement results of the XRD pattern for MZZ–NM.

Cathode	Actual elemental ratios					
	Na	Ni	Mn	Mg	Zn	Zr
NM	0.644	0.317	0.648			
MZZ–NM	0.640	0.273	0.621	0.021	0.026	0.024

Table S3. ICP-AES measurements for NM and MZZ–NM.

Materials	Voltage range (V, vs. Na/Na^+)	Capacity retention , C-rate, cycles	Discharge capacity ($mAh \cdot g^{-1}$)	Refs.
$Na_{0.67}Ni_{0.28}Mg_{0.025}Zn_{0.025}Mn_{0.62}Zr_{0.05}O_2$	2.0-4.4	79.1%,5C,700	96.1	This work
$Na_{0.76}Ni_{0.23}Cu_{0.075}Zn_{0.075}Mn_{0.62}O_2$	2.0-4.5	73.1%,5C,500	82.1	2
$Na_{0.67}Ni_{0.33}Mn_{0.67}O_2$@Zr-1.5%	2.0-4.5	77%,5C,200	111.3	3
$Na_{0.67}Ni_{0.25}Mg_{0.083}Mn_{0.55}Ti_{0.117}O_2$	3.0–4.4	77%,2C,200	84	4
$Na_{0.7}Ni_{0.2}Fe_{0.2}Mn_{0.5}Zn_{0.1}O_2$	2.4–4.5	71.6%,5C,300	106.9	5
$Na_{0.62}K_{0.05}Fe_{0.5}Mn_{0.5}O_2$	2.0-4.0	72%,3C,200	81	6
$Na_{0.65}Mn_{0.65}Cu_{0.2}Li_{0.06}Mg_{0.015}Ti_{0.015}Al_{0.015}Zr_{0.015}Y_{0.015}La_{0.015}O_2$	2.0–4.5	87%,1C,100	97.8	7
$Na_{0.85}Li_{0.12}Ni_{0.198}Be_{0.011}Mg_{0.011}Mn_{0.66}O_2$	2.0-4.3	78.3%,5C,300	75.2	8
$Na_{2/3}Li_{1/6}Fe_{1/6}Co_{1/6}Ni_{1/6}Mn_{1/3}O_2$	2.0–4.5	63.7%,5C,300	112	9

Table S4. Comparison of Half-Cell Performance in Layered Oxides for Sodium-Ion Batteries.

Samlpe	$D_{Na+}/cm^2\ s^{-1}$								
	PeakA1	PeakC1	PeakA2	PeakC2	PeakA3	PeakC3	PeakA4	PeakC4	PeakA5
NM			6.17198E-12	5.07409E-12					
MZZ–NM	1.75843E-11	1.18963E-10	1.56866E-09	1.03794E-09	1.62005E-09	1.65215E-09	1.11248E-11	1.52312E-11	3.41461E-12

Table S5. Sodium ion diffusion coefficients (D_{Na+}) of the redox peaks for NM and MZZ–NM.

Electrodes	Rsf [Ω]	Rct [Ω]
NM	567	15262
MZZ–NM	453.4	5557

Table S6. Fitted parameters of the Nyquist plots for NM and MZZ–NM.

Full cell	Voltage (V)	Specific energy $Wh \cdot kg^{-1}$	Capacity retention, cycles	Current $mA \cdot g^{-1}$	Refs.
$Na_{0.67}Ni_{0.28}Mg_{0.025}Zn_{0.025}Mn_{0.62}Zr_{0.05}O_2$ //HC	2.0-4.4	321.6	84.7%,100	170	This work
$Na_{0.67}Ni_{0.28}Mg_{0.04}Al_{0.02}Mn_{0.64}Ti_{0.02}O_2$ //HC	1.9-4.3	258.8	91.6%,50	34	10
$Na_{0.67}Ni_{0.33}Mn_{0.67}O_2$@Zr-1.5%//HC	2.0-3.7		74%,200	17.3	4
$Na_{0.67}Ni_{0.28}Zn_{0.05}Mn_{0.62}Ti_{0.05}O_{1.95}F_{0.05}$//HC	2.0-4.35		66.1%,100	170	11
$Na_{0.61}Ca_{0.05}[Li_{0.1}Ni_{0.23}Mn_{0.67}]O_{1.95}F_{0.05}$//HC	1.4-4.2	273(16 $mA \cdot g^{-1}$)	92.4%,100	80	12
$NaNi_{0.25}Mg_{0.05}Cu_{0.1}Fe_{0.2}Mn_{0.2}Ti_{0.1}Sn_{0.1}O_2$// HC	1.0-4.0	260(14 $mA \cdot g^{-1}$)	76.5%,500	70	13
$Na_{0.8}Cu_{0.22}Li_{0.08}Mn_{0.67}O_2$//HC	1.9-4.3	292.3(13 $mA \cdot g^{-1}$)	93%,150	130	14
$NaNi_{0.305}Fe_{0.33}Mn_{0.33}Ce_{0.025}O_2$//HC	1.5-4.0		82%,100	120	15

Table S7. Comparison of Full-Cell Performance in Layered Oxides for Sodium-Ion Batteries.

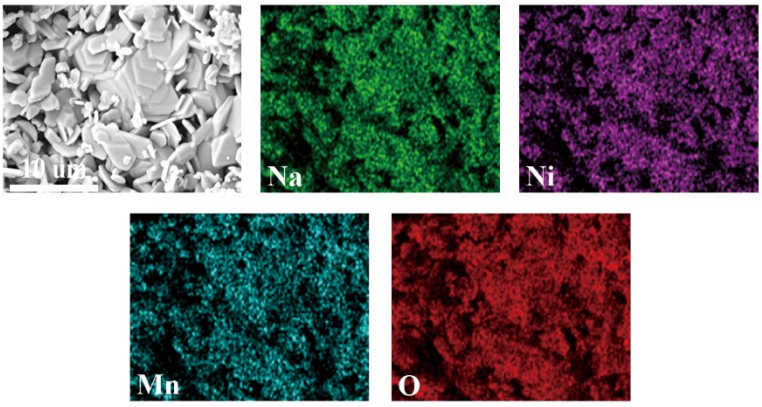

Figure S1. The microscopic morphology and element distribution of NM.

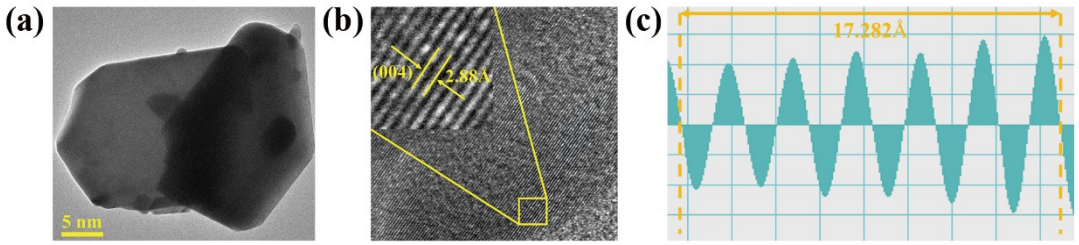

Figure S2. The TEM (a), SAED (b) of MZC–NM. Lattice spacing measurement diagram (c) of MZZ–NM.

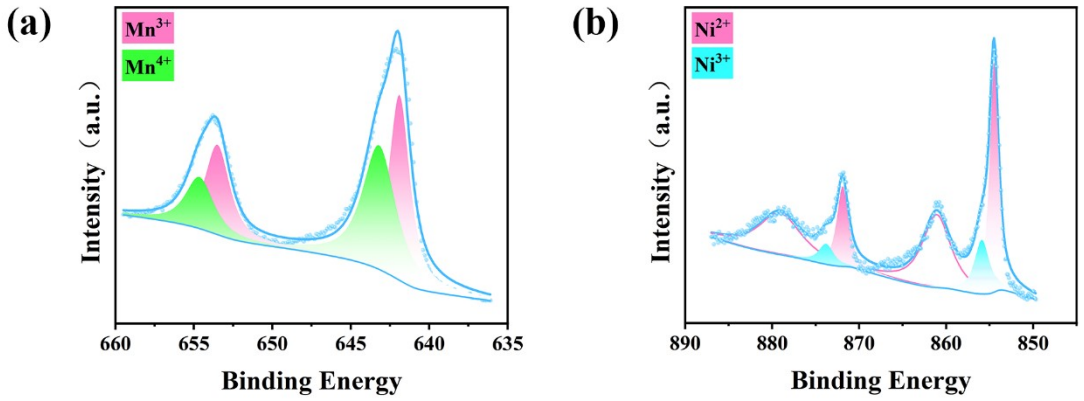

Figure S3. XPS spectra of NM. (a) Mn; (b) Ni.

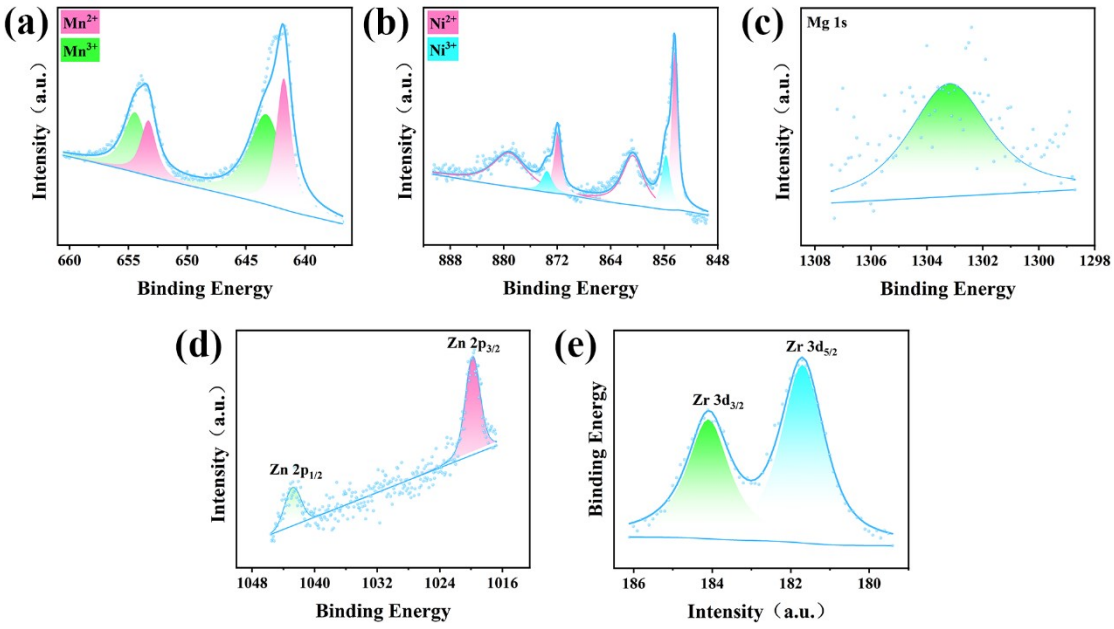

Figure S4. XPS spectra of MZZ–NM. (a) Mn; (b) Ni; (c) Mg; (d) Zn;(e) Zr.

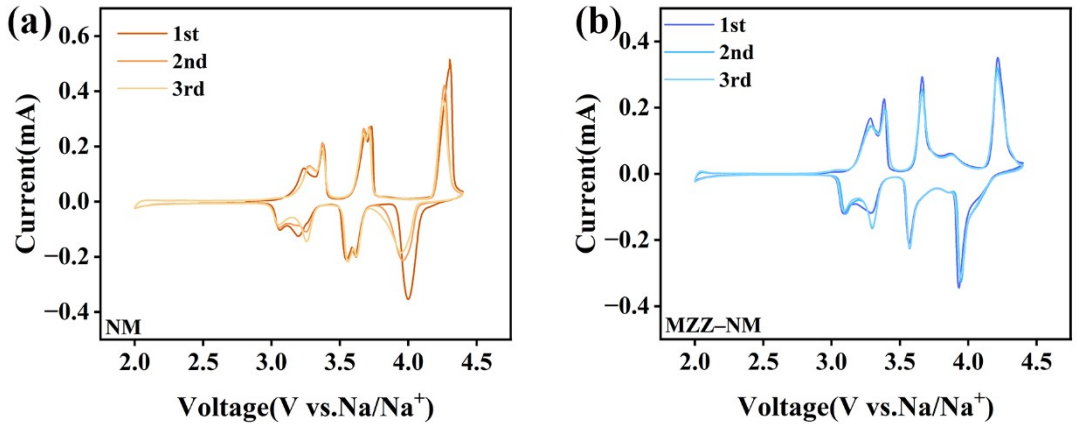

Figure S5. Cycling Voltammetry (CV) curves of (a) NM and (b) MZZ–NM in the first three cycles at 0.1mV·s^{-1} scanning rates.

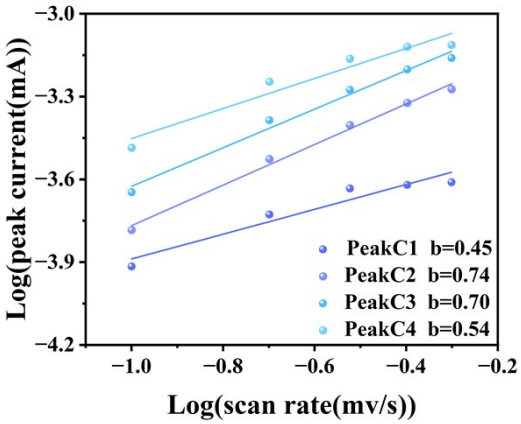

Figure S6. The b-value for the reduction peak of MZZ–NM derived from CV curves at various scan rates.

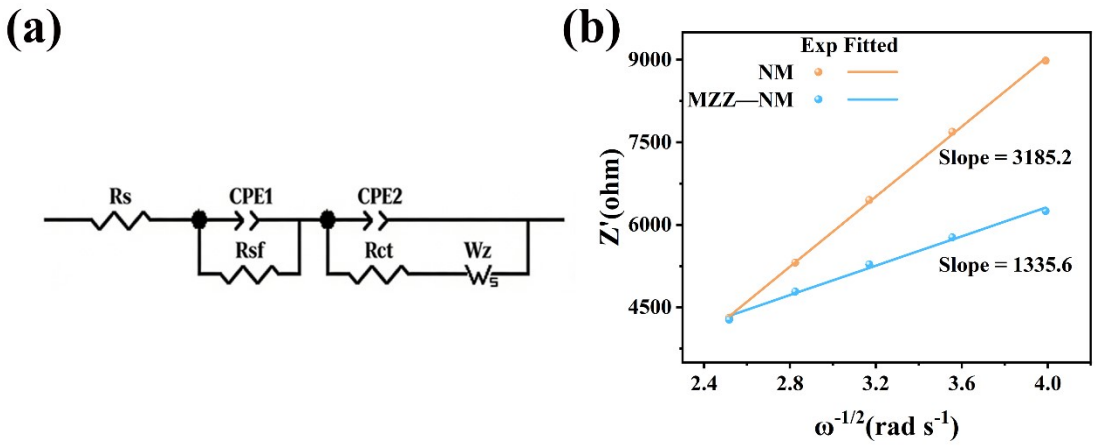

Figure S7. a) The equivalent circuit model used to fit the Nyquist plots and b) the mathematical relationship between Z and $\omega^{-1/2}$ of the NM, and MZZ–NM.

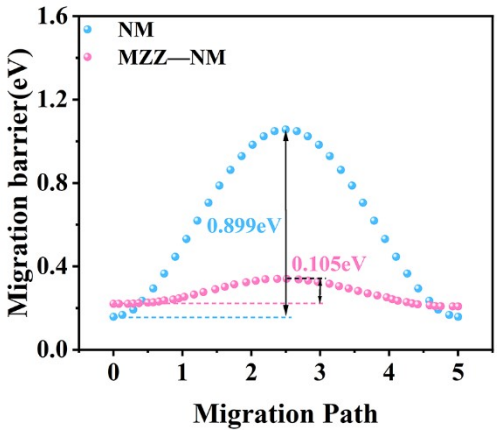

Figure S8. Migration energy barriers for Na^+ diffusion in NM and MZZ–NM.

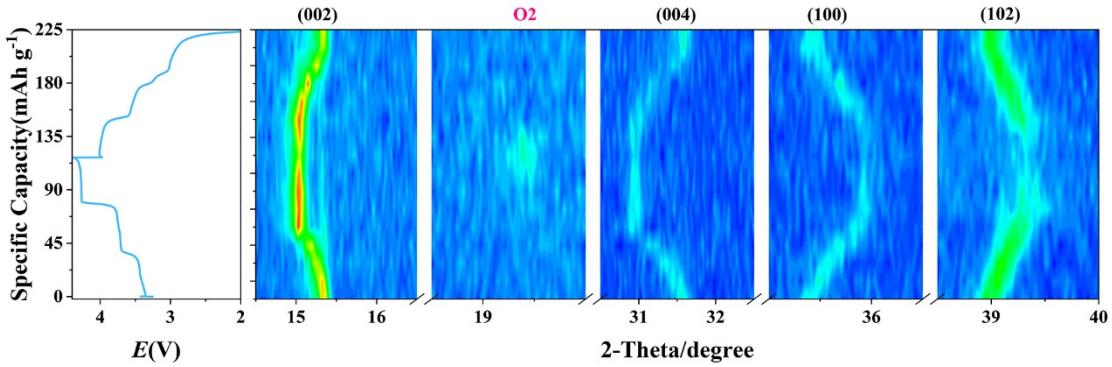

Figure S9. In-situ XRD contour map of NM.

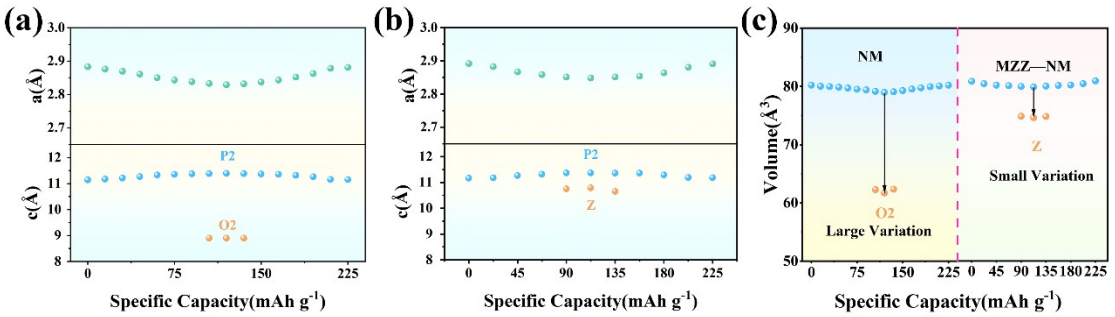

Figure S10. Evolution of the a-axis and c-axis lattice parameters for (a) NM and (b) MZZ–NM during the first charge-discharge cycle. (c) The calculated volume of both samples during the first charging/discharging cycle.

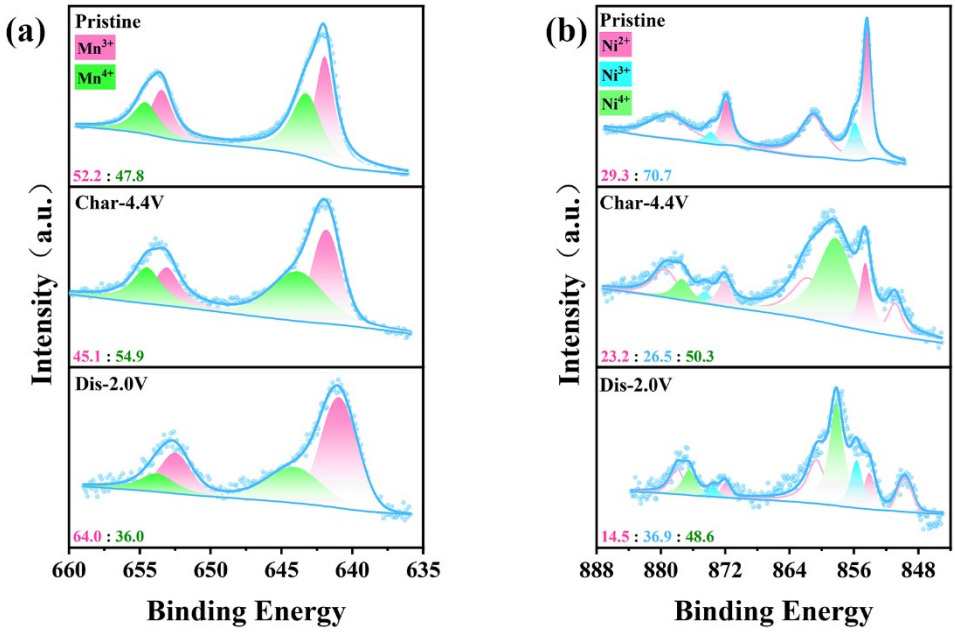

Figure S11. XPS spectra of the (a) Mn 2p, and (b) Ni 2p for the NM in the pristine state, after charging to 4.4 V, and after discharging to 2.0 V.

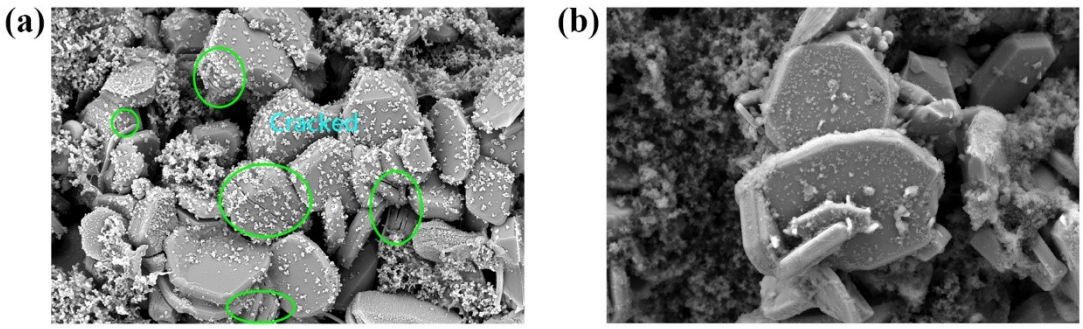

Figure S12. SEM image of (a) NM and (b) MZZ–NM after 200 cycles in the voltage range of 2–4.4 V at 5C.

References

1 L. L. Wong, K. C. Phuah, R. Dai, H. Chen, W. S. Chew and S. Adams, Chem. Mater., 2021, **33**, 625-641.

2 H. Fan, H. Jin, Y. Shang, Y. Wang, J. Yang, H. Chen, X. Xiao, Y. Yang, J. Wu, S. Peng and D. Yan, Chem. Eng. J., 2025, **503**, 158662.

3 H. Ren, L. Zheng, Y. Li, Q. Ni, J. Qian, Y. Li, Q. Li, M. Liu, Y. Bai, S. Weng, X.

Wang, F. Wu and C. Wu, Nano Energy., 2022, **103**, 107765.

4 Y. Huang, Z. Yan, W. Luo, Z. Hu, G. Liu, L. Zhang, X. Yang, M. Ou, W. Liu, L. Huang, H. Lin, C.-T. Chen, J. Luo, S. Li, J. Han, S. Chou and Y. Huang, Energy Storage Mater., 2020, **29**, 182-189.

5 H. Wang, H. Chen, Y. Mei, J. Gao, L. Ni, N. Hong, B. Zhang, F. Zhu, J. Huang, K. Wang, W. Deng, D. S. Silvester, C. E. Banks, S. Yasar, B. Song, G. Zou, H. Hou and X. Ji, ACS Nano., 2024, **18**, 13150-13163.

6 G. Tang, Z. Chen, Z. Lin, S. Luo, T. Chen, J. Chen, W. Xiang, W. Li and M. Chen, J. Alloys Compd., 2023, **947**, 169482.

7 Z. Wang, L. Fang, X. Fu, S. Zhang, H. Kong, H. Chen and F. Fu, Chem. Eng. J., 2024, **480**, 148130.

8 H. Liu, Y. Wang, X. Ding, Y. Wang, F. Wu and H. Gao, Sustainable Energy & Fuels., 2024, **8**, 1304-1313.

9 L. Yao, P. Zou, C. Wang, J. Jiang, L. Ma, S. Tan, K. A. Beyer, F. Xu, E. Hu and H. L. Xin, Adv. Energy Mater., 2022, **12**, 2201989.

10 B. Peng, Z. Zhou, J. Shi, S. Xu, J. Yang, C. Xu, D. Zuo, J. Xu, L. Ma, S. Guo and H. Zhou, Angew. Chem., Int. Ed., 2024, **63**, e202411618.

11 Y. Fan, X. Ye, X. Yang, L. Guan, C. Chen, H. Wang and X. Ding, J. Mater. Chem. A., 2023, **11**, 3608-3615.

12 X. Liu, C. Yuan, X. Zheng, G. Cheng, H. Qian, B. Zheng, X. Lu, Y. Yang, Y. Zhu and Y. Xiang, Adv. Mater., 2024, **36**, 2407519.

13 F. Ding, C. Zhao, D. Xiao, X. Rong, H. Wang, Y. Li, Y. Yang, Y. Lu and Y.-S. Hu, J. Am. Chem. Soc., 2022, **144**, 8286-8295.

14 Y. Wang, J. Jin, X. Zhao, Q. Shen, X. Qu, L. Jiao and Y. Liu, Angewandte Chemie., 2024, **136**, e202409152.

15 Y. Li, L. Lei, J. Hou, G. Wang, Q. Ren, Q. Shi, J. Wang, L. Chen, G. Zu, S. Li, J. Wu, Y. Xu and Y. Zhao, J. Energy Chem., 2025, **105**, 224-232.